Separation and Purification Technology 230 (2020) 115858

Contents lists available at ScienceDirect

Separation and Purification Technology

journal homepage: www.elsevier.com/locate/seppur

# High-pressure $CO_2/CH_4$ separation of Zr-MOFs based mixed matrix membranes

Mohd Zamidi Ahmad[a,b,c,1], Thijs A. Peters[d], Nora M. Konnertz[e], Tymen Visser[e], Carlos Téllez[c], Joaquín Coronas[c], Vlastimil Fila[a], Wiebe M. de Vos[b], Nieck E. Benes[b,*]

[a] Department of Inorganic Technology, University of Chemistry and Technology Prague, Technicka 5, Dejvice – Praha 6, 16628 Prague, Czech Republic
[b] Membrane Science and Technology, Faculty of Science and Technology, MESA+ Institute for Nanotechnology, University of Twente, P.O. Box 217, AE Enschede, Netherlands
[c] Chemical and Environmental Engineering Department and Instituto de Nanociencia de Aragón (INA) and Instituto de Ciencia de Materiales de Aragón (ICMA), Universidad de Zaragoza-CSIC, 50018 Zaragoza, Spain
[d] SINTEF Industry, P.O. Box 124, Blindern, N-0314 Oslo, Norway
[e] European Membrane Institute Twente (EMI), Faculty of Science and Technology, University of Twente, P.O. Box 217, AE Enschede, Netherlands

ARTICLE INFO

*Keywords:*
Zr-based MOF
Mixed matrix membrane
High-pressure separation
$CO_2$ capture
$H_2S$ separation

ABSTRACT

The gas separation properties of 6FDA-DAM mixed matrix membranes (MMMs) with three types of zirconium-based metal organic framework nanoparticles (MOF NPs, ca. 40 nm) have been investigated up to 20 bar. Both NPs preparation and MMMs development were presented in an earlier publication that reported outstanding $CO_2/CH_4$ separation performances (50:50 vol% $CO_2/CH_4$ feed at 2 bar pressure difference, 35 °C) and this subsequent study is to demonstrate its usefulness to the natural gas separation application. In the current work, $CO_2/CH_4$ separation has been investigated at high pressure (2–20 bar feed pressure) with different $CO_2$ content in the feed (10–50 vol%) in the temperature range 35–55 °C. Moreover, the plasticization, competitive sorption effects, and separation of the acid gas hydrogen sulfide ($H_2S$) have been investigated in a ternary feed mixture of $CO_2$:$H_2S$:$CH_4$ (vol% ratio of 30:5:65) at 20 bar and 35 °C. The incorporation of the Zr-MOFs in 6FDA-DAM enhances both $CO_2$ permeability and $CO_2/CH_4$ selectivity of this polymer. These MMMs exhibit high stability under separation conditions relevant to an actual natural gas sweetening process. The presence of $H_2S$ does not induce plasticization but increases the total acid gas permeability, acid gas/$CH_4$ selectivity and only causes reversible competitive sorption. The overall study suggests a large potential for 6FDA-DAM Zr-MOF MMMs to be applied in natural gas sweetening, with good performance and stability under the relevant process conditions.

## 1. Introduction

The acid gas content (carbon dioxide, $CO_2$; hydrogen sulfide, $H_2S$) in raw natural gas varies accordingly to the hydrocarbon geo-origins [1,2] and is commonly in the range of 25–55 mol.% for $CO_2$ and below 2 mol.% for $H_2S$ (≥ 5 mol.% in several regions) [3,4]. $CO_2$, the most undesirable diluent aside from $H_2S$, is essential to be discarded from the gas stream as it corrodes transmission pipelines in the presence of water [5,6]. Additionally, $CO_2$ lowers the natural gas caloric value and causes atmospheric pollution [2,3,5]. Consequently, the content of these impurities must be reduced to meet the industrial processing and pipeline distribution requirements, e.g., maximum allowable contents of 2–3 mol.% $CO_2$ and 0.0004–0.0005 mol.% (4.3–5.0 ppm) $H_2S$ (see Table S1) [7]. In the last decades, the advances in gas separation membranes have allowed the technology to increase its share of the total membrane market, comprising over 1000–1500 million US dollar per year [8] and appear to be the most viable alternative to substitute the conventional highly energy consuming processes, including the solvent-based adsorption processes [5]. However, due to challenges such as plasticization especially at high-pressure operation and degradation, membrane processes only represents < 5% of the natural gas sweetening market [9,10].

Both plasticization and degradation effects can be suppressed by polymer blending and cross-linking [11–15], but a more promising method is the combination of polymeric and inorganic materials as mixed matrix membranes (MMMs) [16–20]. Yong et al. [16] reported the effectiveness of 2 wt% POSS (polyhedral oligomeric silsesquioxane) nanoparticles into the highly permeable PIM-1 to suppress the neat

* Corresponding author.
*E-mail address:* n.e.benes@utwente.nl (N.E. Benes).
[1] Current address: Organic Materials Innovation Center (OMIC), School of Chemistry, University of Manchester, Oxford Rd, M13 9PL Manchester, United Kingdom.

https://doi.org/10.1016/j.seppur.2019.115858
Received 25 June 2019; Received in revised form 24 July 2019; Accepted 24 July 2019
Available online 25 July 2019

polymer $CO_2$-induced plasticization pressure of 15 bar in the range of tested pressure (30 bar) with 50:50 vol% $CO_2$:$CH_4$ feed mixture, at 35 °C. Additionally, the MMM presented 40.8% $CO_2$ permeability and 11.4% $CO_2/CH_4$ selectivity improvements. Adams et al. [17] reported a more than five times increase of $CO_2$ partial pressure needed to plasticize PVAc-50 wt% zeolite 4A at 30 bar, also measured with 50:50 vol % $CO_2$:$CH_4$ feed mixture, at 35 °C. Both Shahid and Nijmeijer [18] and Samadi and Navarchian [19] reported higher $CO_2$-plasticization pressures of Matrimid® 5218 (neat $P_{plasticization.}$ of ~10 bar) by incorporating 30 wt% mesoporous Fe-BTC [18], 5 wt% MgO [19] and 10 wt% modified clay mineral with polyaniline [19], up to 21, 15 and 30 bar, respectively.

Permeation of a mixture of gases through a membrane can depend strongly on the operating parameters, for example, the feed pressure and temperature, amongst others due to the gases' non-ideal behavior [21–23] and their competitive sorption [21,23–25]. Moreover, in a MMM system, the presence of a porous filler and the new filler-polymer interfacial phase created need to be understood as they further influence the gas mobility and sorption through the membrane. Metal organic frameworks (MOFs), formed with metal-based clusters linked by organic ligands [26] in three-dimensional crystalline frameworks with permanent porosity, are an emerging class of porous fillers [27]. They have gained substantial attention due to their high $CO_2$ uptake (i.e., HKUST-1 of 7.2 mmol·g$^{-1}$ [28], MOF-74 of 4.9 mmol·g$^{-1}$ [29], at 1 bar, 273–298 K), large surface areas up to 7000 m$^2$·g$^{-1}$ [30], well-defined selective pores due to their crystallinity, amongst other features. Many researchers observed that the incorporation of a MOF into the polymer continuous phase improved not only its separation properties but also its physical properties [16,31–33], due to interfacial interactions between the polymer and the MOFs. The polymer, in some cases, penetrates the MOF open pores or rigidifies and forms microvoids at the interface [34,35], thereby affecting the membrane's physical properties and gas separation performance.

Zr-based MOF UiO-66 is a highly stable new material and has recently been applied as part of a MMM [31,36,37]. The synthesis of three types of Zr-MOFs, namely UiO-66 and its functionalized derivatives, UiO-66-$NH_2$ and UiO-66-NH-$COCH_3$, as well as MMM fabrication with 6FDA-DAM have been presented earlier [31,34]. In the current paper, we present the gas separation performance of the neat 6FDA-DAM membranes and their derived Zr-MOF MMMs as a function of feed pressure between 2 and 20 bar. At the highest pressure, the effects of $CO_2$ content in the feed mixture on membrane performance have been investigated, at various temperatures (35–55 °C). Finally, the presence of $H_2S$ to the separation performances has been studied.

## 2. Experimental

### 2.1. Materials and membrane fabrications

The UiO-66 and UiO-66-$NH_2$ NPs (ca. 40 nm in size) were synthesized accordingly to Hou et al. [38], at 1 to 1 M ratio of zirconium (IV) chloride ($ZrCl_4$, ≥99.5% trace metal basis) to 1,4-benzenedicarboxylic acid (BDC, 98%) or 2-amino-1,4-benxenedicarboxylic acid ($NH_2$-BDC, 99%), in *N,N*-dimethylformamide (DMF, ≥99.9%), through a solvothermal process in a pre-heated oven at 120 °C/24 h for UiO-66 and at 80 °C/14 h for UiO-66-$NH_2$. A second heating step was conducted for UiO-66-$NH_2$ at 100 °C for 24 h. UiO-66 was activated by thermal treatment in a furnace at 300 °C for 3 h, with a heating rate of 15 °C·min$^{-1}$, whereas chemical activation was conducted for UiO-66-$NH_2$, where the precipitated NPs were washed in an absolute ethanol bath at 60 °C, three times in three days (ethanol was changed daily). After the complete cycle, the NPs were dried at room temperature. A covalent post-synthetic modification (PSM) was conducted onto UiO-66-$NH_2$ to produce UiO-66-NH-$COCH_3$ in chloroform ($CHCl_3$, anhydrous ≥99%) and acetic anhydride ($AcO_2$, ACS Reagent, ≥98.0%) solution, under reflux at 55 °C/24 h. Once completed, the colloidal solution was centrifuged, rinsed with fresh $CHCl_3$ (15 mL, 3x) and dried overnight at 150 °C before characterization and use. The conversion yield was determined by the percentage of amide groups present in the modified NPs using proton nuclear magnetic resonance ($^1$H NMR), and the digestion method was presented elsewhere [38,39]. All reactants applied in the NP synthesis were supplied by Sigma-Aldrich.

6FDA-DAM (Mw = 418 kDa) was purchased from Akron Polymer Systems, Inc. and dried overnight at 100 °C before use. Pure polymer membranes ("neat") and MMMs were fabricated by dissolving the corresponding amount of 6FDA-DAM in chloroform, making a dope solution of 10 wt%. In the case of MMM, a priming step was conducted with 10–15 wt% of the total polymer weight that proves to improve the inorganic filler dispersion in the continuous polymer phase [40–42]. The final dope solutions were casted in a Petri dish and covered for controlled solvent evaporation overnight before being treated at 110 °C before subsequent characterization and permeation measurements. The flat sheet membranes were in the thickness range of 100–150 µm.

### 2.2. Standard permeation measurement

To assess the gas separation performance of the membranes, a 25/25 cm$^3$(STP)·min$^{-1}$ $CO_2/CH_4$ binary feed mixture was used at a pressure difference of 2 bar at 35 °C applying He as sweep gas at 1 cm$^3$(STP)·min$^{-1}$. The permeate composition was analyzed online by an Agilent 3000A micro-GC equipped with a thermal conductivity detector (TCD) at the Institute Nanoscience of Aragon (INA), University of Zaragoza. The membrane module is as described elsewhere [43]. The permeability was calculated as the penetrated gas flux, normalized for the membrane thickness and the partial pressure drop across the membrane, and presented in Barrer (1 Barrer = 10$^{-10}$ cm$^3$(STP)·cm·cm$^{-2}$·s$^{-1}$·cmHg$^{-1}$ (Eq. (1)).

$$Permeability,\quad P_{gas} = \frac{Flux_{gas}\,(cm^3(STP).\ cm^{-2}.\ s^{-1}) \times Thickness\,(cm)}{\Delta p_{gas}\,(cm.\ Hg)} \tag{1}$$

The separation factor ($\alpha$) of two competing gases was calculated using Eq. (2), considering the mole fraction ($x$) of gas $i$ and $j$ in both feed and permeate streams. The mixed gas separation performance was previously discussed [34], and the best performing MMMs are with 14–16 wt% Zr-MOF particle loadings.

$$\alpha_{i/j} = \frac{x_i^{perm.}/x_j^{perm.}}{x_i^{feed}/x_j^{feed}} \tag{6-2}$$

### 2.3. High-pressure performance evaluation

The membranes were placed in a proprietary high-pressure permeation module obtained from the European Membrane Institute (EMI, The Netherlands). The membrane was supported with an S&S 589/1 black ribbon ash-less filter paper on a perforated plate to avoid membrane deformation during the high-pressure testing. The sample was sealed with an o-ring system providing for an effective membrane area of 0.78 cm$^2$. Both feed and retentate sides were connected by high-pressure Swagelok quick-connects whereas the permeate gas was collected using a 1/8 in. Swagelok connector.

The permeation module was placed inside a Memmert UF450 forced air circulation oven, connected to a proprietary high-pressure permeation set-up at SINTEF Materials and Chemistry, Oslo for gas separation measurement (Fig. 1). The permeation set-up is designed to withstand pressures up to 92 bar with a forced air temperature control up to 300 °C. The feed (150 cm$^3$(STP)·min$^{-1}$) and permeate (10 cm$^3$(STP)·min$^{-1}$) flow rates were controlled by automated Bronkhorst High-Tech mass controllers (MFC), equipped with a back pressure controller (Bronkhorst High-Tech, P-512C equipped with an F-033C control valve, max of 92 bars) on the feed side for pressure

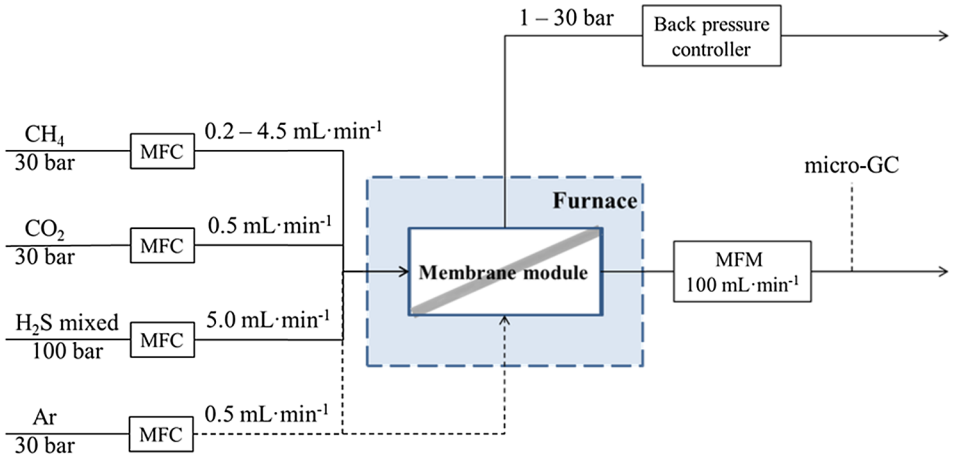


**Fig. 1.** Schematic representation of the high-pressure experimental set-up. The mass flows are calibrated at standard temperature and pressure condition.

**Table 1**
$CO_2$, $CH_4$ permeability and $CO_2/CH_4$ selectivity of neat 6FDA-DAM and its Zr-MOF MMMs, measured 35 °C, at a pressure difference of 2 bar with an equimolar binary mixture of $CO_2$ and $CH_4$.

| Membrane | Gas permeability (Barrer) | | $CO_2/CH_4$ Selectivity |
|---|---|---|---|
| | $CO_2$ | $CH_4$ | |
| Neat | 335 | 17.7 | 19.3 |
| MMM UiO-66 14 wt% | 888 | 35.9 | 25.1 |
| MMM UiO-66-$NH_2$ 16 wt% | 521 | 21.9 | 23.8 |
| MMM UiO-66-NH-$COCH_3$ 16 wt% | 459 | 18.1 | 25.4 |

regulation. The atmospheric-pressure permeate gas analyzed by a two-channel column (MolSieve 5A, MS5 and PoraPLOT U, PPU) Agilent 490 micro-GC, coupled with thermal conductivity detectors (TCD). The micro-GC was calibrated for low $CO_2$ (0–12 vol%), $CH_4$ (0–5 vol%) and $H_2S$ (0–0.5 vol%) concentrations in argon. Good correlation coefficients of $R^2 = \geq 0.999$ were obtained for the μ-GC response as a function of $CO_2$, $CH_4$, and $H_2S$ concentration. The fluxes were calculated from the measured permeate concentrations and the calibrated flow of Ar sweep gas.

High-pressure gas permeation measurements were conducted accordingly to the following experimental sequence, and the separation performances were calculated correspondingly to Eqs. (1) and (2).

1. Pressure variation with 50:50 vol% $CO_2$: $CH_4$ feed mixture: Preliminary measurement at 2 bar and 35 °C was conducted to validate the initial membrane performances, and the pressure was subsequently increased to 5 and 10 bar. Before proceeding to 20 bar, the $CO_2$ feed content was decreased to 10 vol% for the second step measurements.
2. $CO_2$ feed content variation at the feed pressure of 20 bar: At 20 bar, the 10 vol% $CO_2$ feed content was subsequently increased to 20 vol %, 30 vol%, and 50 vol% with $CH_4$.
3. The effect of temperature variation on the separation performance, with 30:70 vol% $CO_2$:$CH_4$ feed mixture at 20 bar: The temperature increase was conducted by stepwise increments from 35 °C to 45 °C and 55 °C, and followed by a reduction back to 35 °C prior to the $H_2S$ introduction (step no. 4).
4. Investigation of separation performance in the presence of $H_2S$ with 30:5:65 vol% $CO_2$:$H_2S$:$CH_4$ feed mixture was conducted at 20 bar and 35 °C.
5. Finally, the $H_2S$ in feed was removed and the system was allowed to purge before the separation efficiency was re-evaluated with 30:70 vol% $CO_2$:$CH_4$ feed mixture, at 20 bar and 35 °C.

It is important to note that the samples were allowed to reach permeation steady-state overnight, after each pressure or feed composition change. Specific attention was given to Health, Safety and Environmental (HSE) matters, and the lab was equipped with preventive safety measures which include $H_2$, CO, and $H_2S$ detection systems, personal portable gas detectors, and separate floor level ventilation suction.

## 3. Results and discussions

In the previous publication [34], we found very promising performance indicators for several 6FDA-DAM MMMs with Zr-MOFs when tested at low pressure (2 bar), with the best performance observed for membranes that contain 14–16 wt% Zr-MOF. An increase in the Zr-MOF loading shows a clear permeability-selectivity trade-off, and selectivity reductions have been observed [34,44]. Table 1 shows the re-measured gas separation performance of the duplicate membranes, at 35 °C, with a pressure difference of 2 bar with an equimolar binary mixture of $CO_2$ and $CH_4$ in SINTEF facility. The permeability values are lower than the published data [34], possibly due to the aging phenomenon which may have occurred during shelf-storage at room temperature for over 250 days. However, the similar improvement trends upon Zr-MOF incorporation were observed. The presence of 14 wt% UiO-66, 16 wt% UiO-66-$NH_2$ and 16 wt% UiO-66-NH-$COCH_3$ improves the $CO_2$ permeability of 6FDA-DAM ($P_{CO2}$ = 335 Barrer) by 165%, 56% and 37%, respectively. These enhancements are well-related to the $CO_2$-philic nature of the Zr-MOFs where a stronger energetic interaction between $CO_2$ (higher quadrupole moment than $CH_4$) and the nanoparticle surfaces at zero coverage, and to the increments in fractional free volume (FFV) in the MMMs (Neat 6FDA-DAM, FFV = 0.238). 14 wt% UiO-66 MMM presents the highest increment value of 39%, followed by 16 wt% UiO-66-$NH_2$ and 16 wt% UiO-66-NH-$COCH_3$ with 16% and 22%, respectively. The $CO_2/CH_4$ selectivity of the samples also increased by 23–32%.

At these observed optimum loadings, the Zr-MOFs addition enhances both $CO_2$ permeability and $CO_2/CH_4$ selectivity tremendously. Besides a higher gas diffusion in the Zr-MOFs, the NPs addition improved the MMM gas diffusivity by inducing an ancillary selective interface phase [45] with additional free volume [46,47]. Agglomeration of the NPs was more prominent at the highest loadings, and the concurrent reduction of the selectivity reduction is likely due to the formation of non-selective by-pass channels in the filler agglomerates [46] and possibly micro-voids in the filler-polymer interface region [41], although such morphological features are not observed by SEM analyses. All the MMMs also presented excellent distribution and inorganic filler-polymer interface interaction (please refer to SEM images, Fig. S5 in the previous publication [34]).

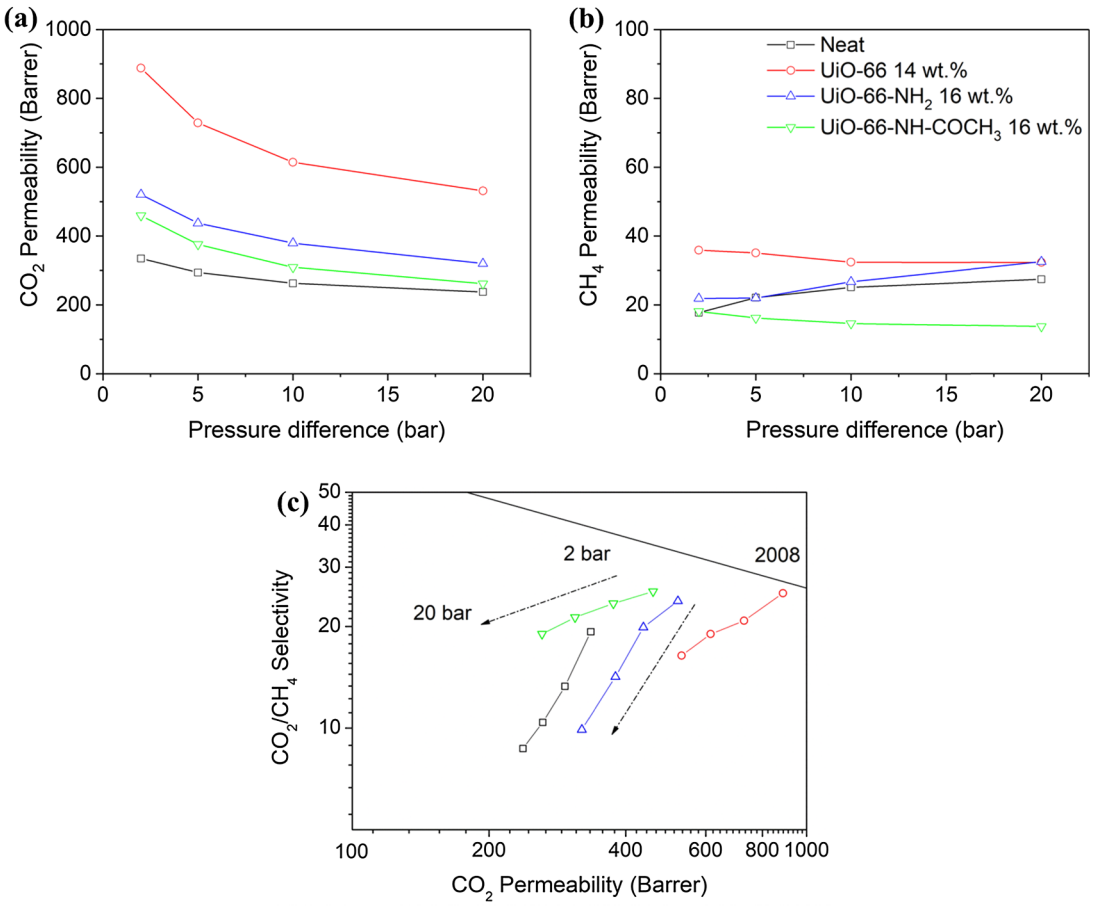


**Fig. 2.** (a) $CO_2$ and (b) $CH_4$ permeabilities of 6FDA-DAM and its Zr-MOFs as a function of feed pressure, measured with 50:50 vol% $CO_2$: $CH_4$ feed mixture at 35 °C. Their corresponding $CO_2/CH_4$ selectivity values are presented in (c), against the 2008 Robeson upper bound [58].

### *3.1. Effect of feed pressure variation to mixed gas separation*

Most of the fundamental studies on Zr-MOF polyimide MMMs related to Matrimid® and 6FDA-copolyimides have been conducted at low pressures where $CO_2$-induced plasticization is expected to be of minor importance [31,48,49]. Here, we have investigated the gas separation performance of 6FDA-DAM and its Zr-MOF MMMs at a pressure ranging from 2 to 20 bar in a 50:50 vol% $CO_2$:$CH_4$ feed mixture at 35 °C. The obtained mixed gas permeability and $CO_2/CH_4$ selectivity behavior as a function of pressure are shown in Fig. 2.

The $CO_2$-induced plasticization pressure is defined to occur at the minimum observed in the $CO_2$-permeability as a function of $CO_2$-partial feed pressure. In the case of mixed gases, the permeation rate of all gases is affected due to swelling of the polymer matrix and the increased chain mobility caused by the high $CO_2$ concentration. The permeation enhancement is more pronounced for the least permeable gases, resulting in a decrease of the selectivity as a function of pressure. In contrast, for all samples in the present study, a monotone decrease in $CO_2$ permeability with increasing pressure is observed (Fig. 2), which does not indicate substantial plasticization [21]. The decrease in $CO_2$ permeability reduction is a result of competitive sorption and the concave shape of the sorption isotherm [25,50]. This constitutes a reduction in driving force for transport with increasing pressure and also gradual saturation of the material may result in lower mobility. Overall, this results is further supported by the clear decrease in permeation coefficient in the polymer matrices (see Fig. S1). The $CO_2$ permeability continuously decreases with increasing pressure indicating there is no apparent $CO_2$-induced plasticization in the thick membrane [21], opposite to the reported single-gas $CO_2$-plasticization pressure of neat 6FDA-DAM membrane between ~10–20 bar, at 35 °C [51,52]. The plasticization pressure differences may be attributed to different physical properties, i.e., molecular weight, density, and polymer free volume, as previously discussed [31,34].

The pressure dependence of the $CH_4$ permeability (Fig. 2(b)) over the measured pressure range, however, suggests that the neat 6FDA-DAM starts to swell immediately after the first pressure increment. It can be explained by dynamic swelling of the polymer matrices upon exposure to the $CO_2$ at high pressure [53], where the penetrating $CO_2$ causes the material dilation and subsequently increases its macromolecular mobility. Several researchers have reported the thermodynamics of swollen glassy polymers by a penetrant [54,55], and a thorough discussion was recently presented by Ogieglo et al. [53] when studying the glassy polymer relaxation in this films. The phenomenon, to the function of pressure, causes extensive dilation of the matrices, influencing the penetrants' permeation. Here, the effect is more apparent in $CH_4$ permeability increase compared to the readily high-permeability $CO_2$. In the case of UiO-66-$NH_2$ MMM, the high $CO_2$-affinity amino functional group increases the $CO_2$ adsorption in the polymer matrixes and directly further influences the molecular dynamic dilation. Even though it is not the membranes' plasticization pressure, their $CO_2/CH_4$ selectivity reduced by 55% and 58% respectively. This behavior also defined as swelling-induced perm-selectivity losses [34], which was observed in several other co-polyimides, such as 6FDA-APAF and TPDA-APAF, when measured with $CO_2/CH_4$ binary mixture up to 25 bar feed pressure, at 35 °C [56]. Heck et al. [57] also observed similar behavior in (6FDA-mPDA)-(6FDA-durene) block co-polyimide, for which they reported an increase in $CH_4$ permeability with pressure (up to 20 bar feed pressure), causing $CO_2/CH_4$ and He/$CH_4$ selectivity

reductions.

The continuous decrease of $CH_4$ permeability in both UiO-66 and UiO-66-NH-$COCH_3$ MMMs demonstrated the competitive sorption effect [59], where $CO_2$ penetrated the membranes' sorption sites which associated to the non-equilibrium free volume in glassy polymer and hindered $CH_4$ to permeate. Polymer plasticization was not observed in these membrane samples.

### 3.2. Effect of $CO_2$ feed composition in high-pressure separation

Fig. S2(a-b) show the $CO_2$ and $CH_4$ permeability of the neat 6FDA-DAM and Zr-MOF MMMs, measured at 20 bar feed pressure and 35 °C, with a different $CO_2$ feed content between 10 and 50 vol%. The significant differences in the initial $CO_2$ permeabilities between the membranes were discussed in the previous publication [34]; higher $CO_2$ permeability in the UiO-66 MMM is attributed to the easiness of $CO_2$ to diffuse into its frameworks, compared to the higher steric hindrance functionalized-MOFs, and also its higher FFV.

The $CO_2$ permeability in the neat 6FDA-DAM and its Zr-MOFs MMMs decreases between 9 and 22%, with the increase of $CO_2$ partial pressure when tested at 20 bar. The lowest reduction of 8.7% was observed for the UiO-66 MMM. The observation, however, is opposite to the previously reported $CO_2$ permeability relationship with $CO_2$ partial pressure at low-pressure measurements, i.e., 6FDA-DAM Zr-MOF MMMs (at 2 bar) [34] and PES/SAPO-34/2-hydroxyl 5-methyl aniline MMMs (at 3 bar) [60]. At the low pressure, a higher $CO_2$ partial pressure produced a more prominent competitive sorption effect, where an increase in $CO_2$ solubility and transport through the membrane medium was observed and inversely decreased the second component's ability to permeate, in this case, $CH_4$.

Evidently, the continuous $CO_2$ permeability reduction with increasing pressure suggests that the competitive sorption effect at high pressure is less influenced by the $CO_2$ partial pressure (see Fig. 3). Instead, it is related to the gradual saturation of permeating gases inside the polymer micro-voids [18]. Nevertheless, a slight increase in the $CH_4$ permeability for the neat membrane (9%) and UiO-66-$NH_2$ MMM (21%) is observed, indicating the possibility of $CO_2$-induced plasticization that started to take effect [61,62]. These samples exhibited the highest $CO_2/CH_4$ selectivity reductions of between 28 and 33% in all the samples (shown in Fig. S2(c), relative to 2008 Robeson's upper bound [58]). Despite this $CH_4$ permeability increment, the behavior can be explained as swelling-induced perm-selectivity losses, an early stage in polymer plasticization [56].

With regard to the initial separation performance (with 10 vol% $CO_2$), similarly to the previous discussion, neat 6FDA-DAM showed a lower $CO_2/CH_4$ selectivity than that of MMMs (UiO-66-$NH_2$ < UiO-66 < UiO-66-$COCH_3$). The proportional selectivity increase in MMMs to the increasing $CO_2$ partial pressure [63–65], which only observed in UiO-66 MMM at the tested feed pressure of 20 bar (3% selectivity increment) represents the membrane's extended $CO_2$ sorption capability due to the $CO_2$-induced plasticization or swelling at constant pressure [63]. Its reduction conversely was explained based on $CO_2$ self-inhibition as a consequence of saturation of the filler active sites at a high $CO_2$ concentration in a feed mixture [60,66]. Referring to that hypothesis, a lower reduction exhibited by UiO-66-NH-$COCH_3$ MMM (13%) compared to UiO-66-$NH_2$ MMM (28%), represented by its lesser concave shape in the permeability isotherm, may be due to a higher $CO_2$ affinity towards acetamide functional groups, with a higher number of adsorption sites compared to UiO-66-$NH_2$ NPs. Moreover, constant selectivity values demonstrate no dependency of an MMM system towards the increasing $CO_2$ partial pressure, as also revealed in the PES/SAPO-34/HMA MMM system, measured at 3 bar [60]. This hypothesis implies that only a minor amount of the active sites is occupied at low pressure.

### 3.3. Effect of operating temperature in the high-pressure separation

Fig. S3(a–c) shows the $CO_2$ and $CH_4$ permeability and the $CO_2/CH_4$ selectivity as a function of the operating temperature applying a 30:70 vol% $CO_2$:$CH_4$ feed mixture at 20 bar. A minor increase in $CO_2$ permeability of < 6% was recorded for all samples, whereas for $CH_4$

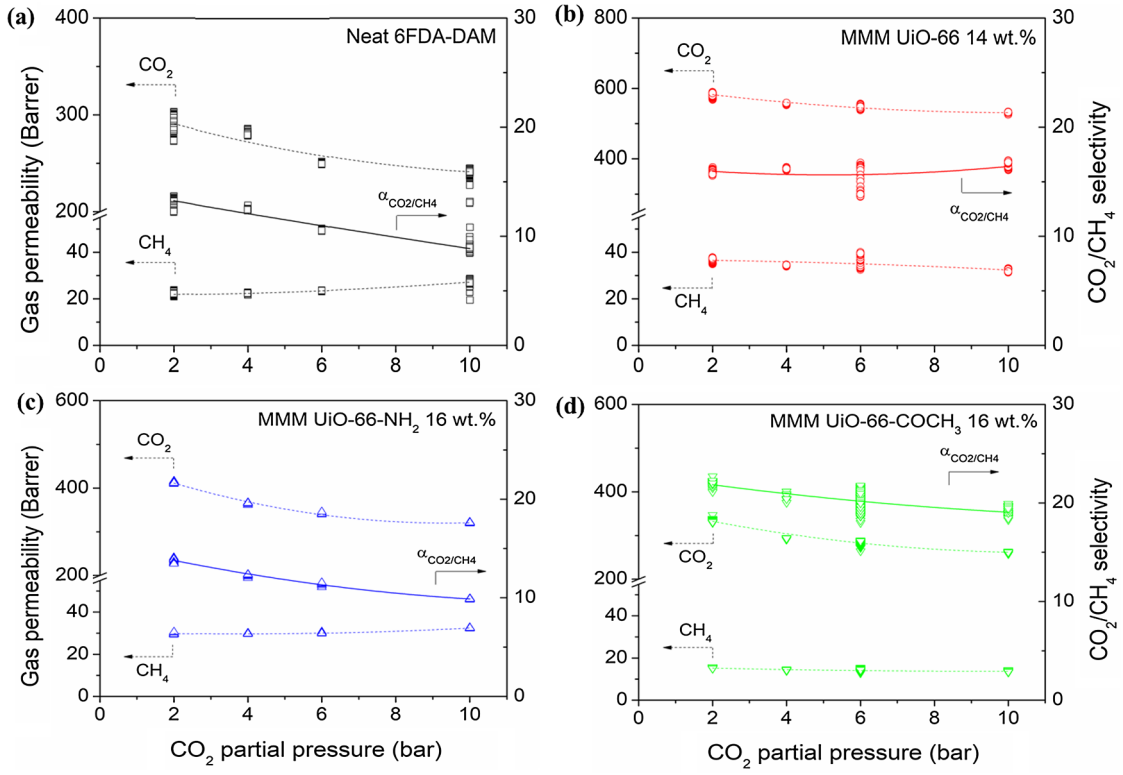


**Fig. 3.** $CO_2$ and $CH_4$ permeabilities, and $CO_2/CH_4$ selectivity of 6FDA-DAM and its Zr-MOF MMMs against $CO_2$ partial pressure, at 20 bar and 35 °C.

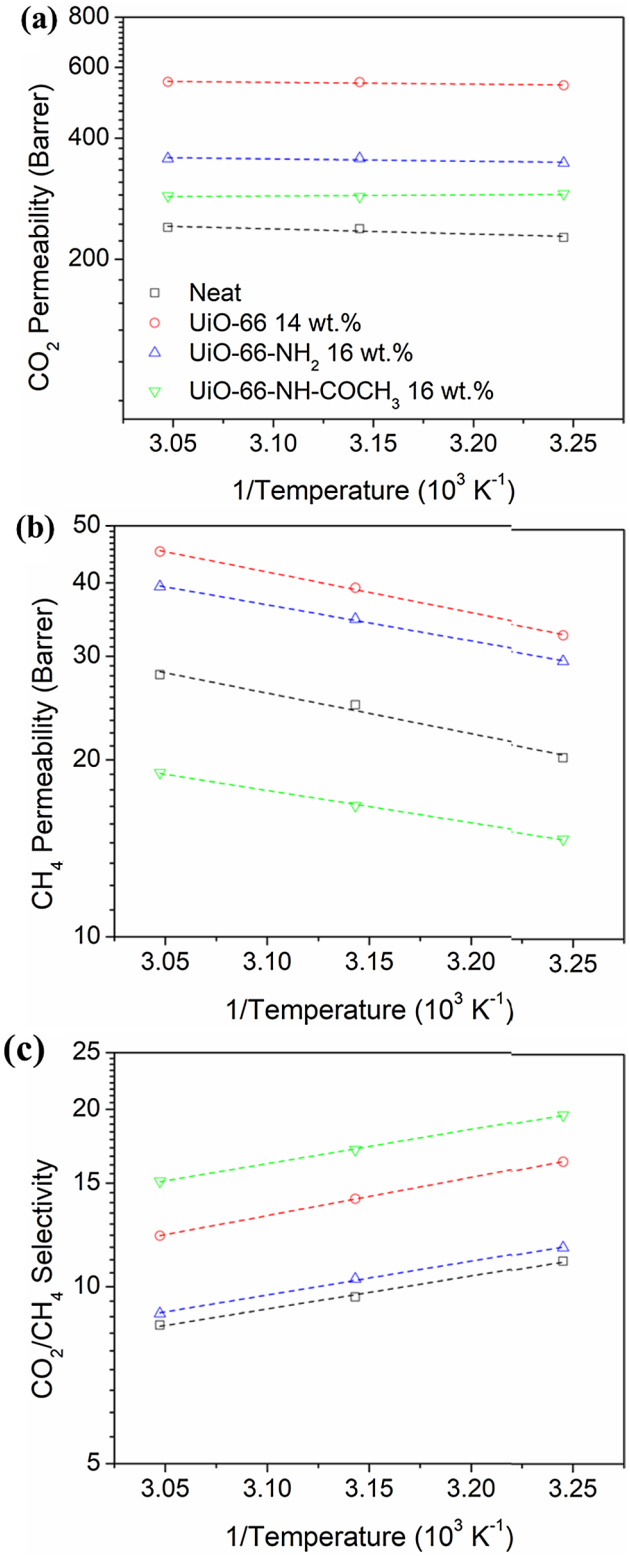


**Fig. 4.** (a) $CO_2$ and (b) $CH_4$ permeability and its (c) perm-selectivity to temperature dependence, for neat 6FDA-DAM and its Zr-MOFs membranes at the measurement temperature of 35–55 °C.

permeability, the increments were higher in between 28 and 37%, as the operating temperature increased from 35 to 55 °C. The effect of temperature on the gas permeability can be quantitatively observed in their activation energy for permeability, following Arrhenius rule using Eq. (3) [67]:

**Table 2**
Activation energy of permeation for $CO_2$ and $CH_4$ in neat 6FDA-DAM and its Zr-MOF MMMs, calculated for the temperature operating range of 35–55 °C, with 30:70 vol% $CO_2/CH_4$ at 20 bar.

| Gas | Membrane | Permeability activation energy, $kJ{\cdot}mol^{-1}$ |
|---|---|---|
| | | $E_a$, (35–55 °C) |
| $CO_2$ | Neat | 0.16 |
| | MMM UiO-66 14 wt% | 0.05 |
| | MMM UiO-66-$NH_2$ 16 wt% | 0.07 |
| | MMM UiO-66-NH-$COCH_3$ 16 wt % | −0.03 |
| $CH_4$ | Neat | 0.85 |
| | MMM UiO-66 14 wt% | 0.86 |
| | MMM UiO-66-$NH_2$ 16 wt% | 0.76 |
| | MMM UiO-66-NH-$COCH_3$ 16 wt % | 0.68 |

$$P = P_0 e^{\frac{-E_a}{RT}} \tag{3}$$

where $P_0$ is a pre-exponential factor of permeation, $E_a$ is activation energy for permeability ($kJ{\cdot}mol^{-1}$), $R$ is the universal gas constant ($8.314\ J{\cdot}mol^{-1}$), and $T$ is the temperature in K. Using $CO_2/CH_4$ selectivity expression of the permeability coefficient ratio of $CO_2$ over $CH_4$, the gas selectivity is defined as the following:

$$\alpha(CO_2/CH_4) = \frac{P_{CO2}}{P_{CH4}} = \frac{P_0(CO_2)}{P_0(CH_4)} \exp\left(-\frac{E_p(CO_2) - E_p(CH_4)}{RT}\right) \tag{4}$$

Fig. 4 indicates that $CH_4$ permeability in the 6FDA-DAM neat membrane and its Zr-MOF MMMs followed Arrhenius rule in the temperature range of 35–55 °C, while the $CO_2$ permeability was less influenced by the temperature. Their permeability coefficients are summarized in Table 2. The permeability dependency is a combination of the diffusion and solubility coefficients temperature dependencies, and the lower $CO_2$ and $CH_4$ activation energies in MMMs as compared to the neat polymer indicate the gas transport through filler porosity [49], and in the interfacial voids on polymer-MOF and MOF-MOF regions which may also reduce the overall permeability $E_a$ of MMMs. Regarding 6FDA-DAM, in addition to polymer matrix compression at the high pressure, the overall $CO_2$ activation energy trend does not show a clear correlation to the membrane FFVs (MMMs (UiO-66; 0.331 > UiO-66-$COCH_3$, 0.292 > UiO-66-$NH_2$; 0.277) > neat 6FDA-DAM, 0.238). Instead, the activation energy seems profoundly influenced by the presence of Zr-MOF nanoparticles in MMMs, in the order of their group functionalities (UiO-66-NH-$COCH_3$ > UiO-66-$NH_2$ > UiO-66 > neat 6FDA-DAM). It also concludes that the $CO_2$ permeation is predominately influenced by its solubility (sorption) in the membrane systems, and less dependent on temperature. The higher activation energies presented by the non-polar $CH_4$ also indicated that its diffusion or transport was more influenced compared to $CO_2$ molecules, giving higher $CH_4$ permeability increments and consequently reduced the $CO_2/CH_4$ selectivity by 22–26%. This observation is also consistent with activated diffusion of non-polar molecules in glassy polymers (related to chain mobility and polymer free volumes) [68], where the least permeable gas often possesses higher activation energy and realizes a more substantial permeability increase with increasing temperature. In any event, the activation energies (temperature-dependent) are low for both the neat polymer membrane and the MMMs, compared to the other 6FDA-based polyimides in the literature (see Table S2). This suggests a low penetrant-membrane interaction perhaps because there is a relatively large difference between the $CO_2$ and $CH_4$ kinetic diameter and the membrane controlling pore size.

Lower $CO_2$ temperature-dependency at this high-pressure separation also indicated by its fugacity coefficient values, closing to 1.0 (ideal

**Table 3**
The compressibility Z factors for $CO_2$ and $CH_4$, calculated using Dranchuk and Abou-Kassem equation of state (DAK – EOS) [69], presented at 35 °C, 45 °C and 55 °C, at 20 bar.

| Temperature, °C | Compressibility Z factor | | Fugacity coefficients, ϕ | | Fugacity (bar) | |
|---|---|---|---|---|---|---|
| | $CO_2$ | $CH_4$ | $CO_2$ | $CH_4$ | $CO_2$ | $CH_4$ |
| 35 | 0.9049 | 0.9699 | 0.9953 | 1.0293 | 19.9051 | 20.5858 |
| 45 | 0.9953 | 0.9735 | 0.9998 | 1.0258 | 19.9953 | 20.5153 |
| 55 | 0.9998 | 0.9767 | 1.0000 | 1.0227 | 19.9998 | 20.4539 |

Calculated from the following constant values and critical state variables:
$CO_2$: gas constant, R = 188.92 J·kg$^{-1}$·K$^{-1}$; isentropic exponent = 1.301; $p_{crit}$ = 73.77 bar; $T_{crit}$ = 30.98 °C.
$CH_4$: gas constant, R = 518.27 J·kg$^{-1}$·K$^{-1}$; isentropic exponent = 1.304; $p_{crit}$ = 45.92 bar; $T_{crit}$ = −82.59 °C.

gas) when temperature is increased (see Fig. S4(a) and S4(b)), proves that the molecule's non-ideal behavior is less influenced by the increasing temperature but predominantly by pressure. It is supported by the fact that $CO_2$ possesses lower fugacity coefficients at the tested separation conditions Table 3 (overall compressibility factor and fugacity coefficient calculated values are presented in Fig. S4). The compressibility factors were determined by an eleven-constant Dranchuk and Abou-Kassem equation of state (DAK-EOS) [69]. The detail is presented in the supporting information document.

Besides that, the $CH_4$ permeability increase was also influenced by the increase of polymer free volume (as a function of polymer chain packing and intersegmental motion) by the effect of elevated temperature. The activated diffusion often proves to be a significant advantage in the separation of non-polar $H_2$ from $CO_2$, giving enhanced $H_2/CO_2$ selectivity at higher temperatures as demonstrated in 6FDA-*m*PBI [68] and PBI-ZIF8 MMMs [70].

$$\log P_0 = \frac{E_p}{R} \times 10^{-3} + Z \quad (5)$$

Regardless of common polymer chemical structures, Van Krevelen [71] presented a positive slope of $1 \times 10^{-3}$ for log $P_0$ and $E_p/R$ plot (Eq. (5)), with Z values of −7.0 and −8.2 for rubbery and glassy polymers respectively, for permeability measurement below their glass transition temperatures. Fig. S5 indicates that the addition of Zr-MOFs into 6FDA-DAM altered $CO_2$ permeability-temperature dependency significantly, giving a negative $E_p/R$ slope of $-0.15 \times 10^{-3}$, while only reduced $CH_4$ permeability-temperature dependency by roughly 70% ($CH_4$ permeability $E_p/R$ slope = $0.32 \times 10^{-3}$).

### 3.4. Effect of the presence of $H_2S$ on membrane separation

The concentration of $H_2S$ in the natural gas mixture varies depending on the geo-origin and can be more than 5 vol% [4,72]. As aforementioned, besides investigating the 6FDA-DAM and its Zr-MOF MMMs performances for $H_2S$ separation, it is important to understand the $H_2S$ effect on membrane performance. We studied the gas separation performance of 6FDA-DAM and its Zr-MOF MMMs with 30:70 vol% $CO_2$:$CH_4$ feed mixture at 20 bar and 35 °C, before adding 5 vol% of $H_2S$, making the feed composition to 30:5:65 vol% $CO_2$:$H_2S$:$CH_4$. The separation performance after $H_2S$ exposure was also investigated and summarized in Table 4.

Upon the addition of 5 vol% $H_2S$ in the mixed gas, $P_{CO2}$ in all samples decreased by an average of 28–34%, accordingly to their functionality order: MMMs (UiO-66-NH-$COCH_3$ > UiO-66-$NH_2$ > UiO-66) > neat 6FDA-DAM. 6FDA-DAM MMMs showed a higher $CO_2$ permeability reduction in the presence of $H_2S$, compared to the neat membrane. The observation exhibited the influence of Zr-MOFs in the MMMs, of which their active metal sites also preferentially adsorb $H_2S$ and thus reduce their $CO_2$ adsorption capacity. $P_{H2S}$ values are in the range of 137–352 Barrer, slightly lower than those of $P_{CO2}$, contributing to the total acid gas permeability of between 304 and 737 Barrer. The increments directly presented the acid gas selectivity over

**Table 4**
Gas separation performances of 6FDA-DAM and its 14–16 wt% Zr-MOFs MMMs, tested with binary (30:70 vol%; $CO_2$:$CH_4$) and tertiary (30:5:65 vol%; $CO_2$:$H_2S$:$CH_4$) feed mixture at 20 bar, 35 °C.

| Feed mixture | Separation performances | 6FDA-DAM membranes | | | |
|---|---|---|---|---|---|
| | | Neat | MMM UiO-66 | MMM UiO-66-$NH_2$ | MMM UiO-66-NH-$COCH_3$ |
| $CO_2$:$CH_4$ | $P_{CO2}$ | 231 | 541 | 359 | 291 |
| (30:70 vol%) | $P_{CH4}$ | 21.7 | 33.0 | 33.1 | 14.8 |
| Before exposure | $\alpha_{CO2/CH4}$ | 10.6 | 16.4 | 10.8 | 19.7 |
| $CO_2$:$H_2S$:$CH_4$ | $P_{CO2}$ | 167 | 385 | 243 | 193 |
| (30:5:65 vol%) | $P_{H2S}$ | 137 | 352 | 224 | 172 |
| | $P_{(CO2+H2S)}$* | 304 | 737 | 466 | 365 |
| | $P_{CH4}$ | 18.5 | 25.4 | 25.7 | 10.6 |
| | $\alpha_{CO2/CH4}$ | 9.1 | 15.2 | 9.5 | 18.2 |
| | $\alpha_{H2S/CH4}$ | 7.4 | 13.6 | 8.7 | 16.2 |
| | $\alpha_{(CO2+H2S)/CH4}$* | 16.4 | 29.0 | 18.1 | 34.4 |
| $CO_2$:$CH_4$ | $P_{CO2}$ | 227 | 543 | 347 | 284 |
| (30:70 vol%) | $P_{CH4}$ | 20.4 | 33.7 | 29.8 | 14.3 |
| After exposure | $\alpha_{CO2/CH4}$ | 11.1 | 16.1 | 11.7 | 19.8 |

Permeability is in Barrer.
* Acid gas, $CO_2$ + $H_2S$.

$CH_4$ of 16.4 for the neat 6FDA-DAM and in the range of 18.1–34.4 for its MMMs. Besides the competitive sorption of a two-component gas mixture, the presence of a third component intensifies the gas mixtures non-ideal behavior and influences each penetrant permeation rate, especially at elevated pressures [21]. Based on gas permeability values, the observed adsorption preference trend is in the order of $CO_2$ > $H_2S$ > $CH_4$, well-agreed to the gasses' isosteric adsorption heat in UiO-66 ($CO_2$; 25.7 kJ·mol$^{-1}$ > $H_2S$; 23.8 kJ·mol$^{-1}$ > $CH_4$; 18.8 kJ·mol$^{-1}$, reported at 30 °C [36]). Functionalized UiO-66 derivatives presented higher values, in the same order. The gas physical properties; dipole moment (Debye), quadrupole moment (au) and polarizability ($a_0^3$), also greatly contributed to the competitive sorption outcomes and $H_2S$ high polarizability explained its higher permeability despite its relatively low content in the feed mixture compared to $CO_2$; $CH_4$: $5.4 \times 10^{-6}$ Debye, 0 au, 17.3 $a_0^3$; $CO_2$: 0 Debye, 3.2 au, 18 $a_0^3$; $H_2S$: 0.978 Debye, 0 au, 25 $a_0^3$ [73]. Hence, the observed $\alpha_{CO2/CH4}$ reduction can be explained by a larger competitive sorption effect induced by $H_2S$ (its solubility is larger than that of $CH_4$) in the membrane systems. In addition to $H_2S$ competitive sorption effect, the reduced $CO_2/CH_4$ selectivity may also be contributed by the fact that $CH_4$ partial pressure in binary mixed gas (70 vol% in feed) is higher than that in ternary system (65 vol% in feed). As a higher $CH_4$ partial pressure will result in its higher permeability, subsequently lowers the $CO_2/CH_4$ selectivity and its competitive sorption effect towards $H_2S$ and $CO_2$ permeability may also not be the same.

In the presence of $H_2S$, all MMMs presented higher $CO_2$, $H_2S$ and acid gas selectivities compared to the neat 6FDA-DAM ($\alpha_{CO2/CH4}$ = 9.1;

**Table 5**
Separation comparison of 6FDA-DAM and its Zr-MOF MMMs with several other dense membranes, when tested with ternary mixed gas feeds containing ≤ 15 mol.% of $H_2S$ at 35 °C.

| Polymer | Pressure (bar) | Feed compositions mol.% ($CO_2$:$H_2S$:$CH_4$) | Permeability (Barrer) | | Selectivity | | Refs. |
|---|---|---|---|---|---|---|---|
| | | | $CO_2$ | $CO_2$ + $H_2S$ | $CO_2/CH_4$ | ($CO_2$ + $H_2S$)/$CH_4$ | |
| 6FDA-DAM | 20 | 30:5:65 | 167 | 304 | 9.1 | 16.4 | This study |
| MMM UiO-66 | 20 | 30:5:65 | 385 | 737 | 15.2 | 29.0 | |
| MMM UiO-66-$NH_2$ | 20 | 30:5:65 | 243 | 466 | 9.5 | 18.1 | |
| MMM UiO-66-NH-$COCH_3$ | 20 | 30:5:65 | 193 | 365 | 18.2 | 34.4 | |
| Cellulose acetate | 10 | 29:6:65 | 2.4 | 4.6 | 22.0 | 41.5 | [77] |
| Pebax 1074 | 10 | 18.1:12.5:69.4 | 155 | 850 | 11.0 | 61.6 | [77] |
| PU2 | 10 | 18.1:12.5:69.4 | 195 | 813 | 5.6 | 23.4 | [77] |
| PIM-6FDA-OH | 34.5 | 15:15:70 | 54.7 | 90.7 | 27.8 | 46.1 | [81] |
| 6FDA-DAM:DABA (3:2) | | | | | | | |
| Annealed at 180 °C | 48 | 20:10:70 | 55.6 | 81.0 | 32.1 | 46.7 | [82] |
| Annealed at 230 °C | 48 | 20:10:70 | 50.8 | 74.4 | 31.1 | 45.5 | [82] |
| 6FDA-DAM | 6.9 | 20:20:60 | 414 | 672 | 24.4 | 39.7 | [79] |

Abbreviation: 6FDA: 2,2-bis(3,4-dicarboxyphenyl)hexafluoropropane diandydride; DAM: 2,4,6-trimethyl-1,3-diaminobenzene; PEBAX: polyether block amide; PU: polyurethane; PIM: polymers of intrinsic microporosity; DABA: 3,5-diaminobenzoic acid.

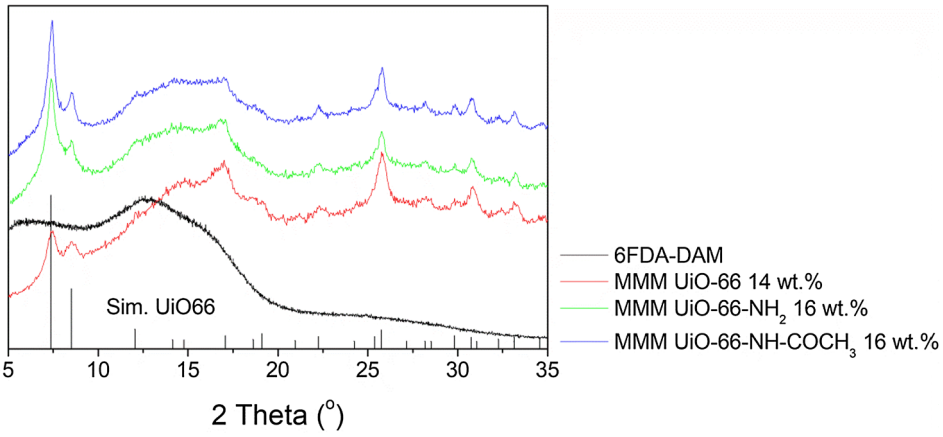


**Fig. 5.** XRD patterns of UiO-66 (simulated [80]), 6FDA-DAM and its Zr-MOF derived MMMs after $H_2S$-exposure in the tertiary mixture (30:5:65 vol%; $CO_2$:$H_2S$:$CH_4$) separation, at 20 bar, 35 °C.

$\alpha_{H2S/CH4}$ = 7.4; $\alpha_{(CO2+H2S)/CH4}$ = 16.4) with the highest values presented in UiO-66-NH-$COCH_3$ MMM ($\alpha_{CO2/CH4}$ = 18.2; $\alpha_{H2S/CH4}$ = 16.2; $\alpha_{(CO2+H2S)/CH4}$ = 34.4). The UiO-66-NH-$COCH_3$ MMM presented similar or higher $\alpha_{H2S/CH4}$ selectivity than several reported membranes, such as in 6FDA-PAI-3/TmPDA (ideal $\alpha_{H2S/CH4}$ = 10.9), Torlon® 4000 T (ideal $\alpha_{H2S/CH4}$ = 14.8), both tested at 4.5 bar, 35 °C [74], and in a rigid (6FDA-mPDA)-(6FDA-durene) block co-polyimide, ($\alpha_{H2S/CH4}$ = ca. 15), tested with 1 vol% $H_2S$ in a $CO_2$:$H_2S$:$N_2$:$CH_4$ quaternary mixture at 3.8 bar, 22 °C [75]. The performance is also comparable to the commercial poly(ester urethane) urea, PEUU, $\alpha_{H2S/CH4}$ = 16 [76] ($CO_2$:$H_2S$:$CH_4$ feed ratio of 5.4:3:remaining, at 55 °C, 20 bar) and cellulose acetate, CA, $\alpha_{(CO2+H2S)/CH4}$ = 41.5 [77] ($CO_2$:$H_2S$:$CH_4$ feed ratio of 29:6:65, at 35 °C, 10 bar). In the separation of an actual natural gas sample containing 5008 ppm $H_2S$, water vapor, $C_1$-$nC_5$, and mercaptan, commercial polyphenylene oxide hollow fibers presented $\alpha_{H2S/CH4}$ = 2.9, while a commercial poly (ester urethane) urea (PEUU) flat sheet membrane gave $\alpha_{H2S/CH4}$ = 3.4, measured at 40 °C and 23 °C, respectively [78]. The separation performances of several other dense membranes to the ternary gas mixture with $H_2S$ at 35 °C are presented in Table 5 for comparison. Most interestingly, Liu *et al.* [79] also demonstrated acid gas permeability and selectivity over $CH_4$ improvement of 6FDA-DAM ($P_{CO2+H2S}$ = 671.8 Barrer, $\alpha_{(CO2+H2S)/CH4}$ = 39.7) by incorporating 30 wt% Y-fum-fcu-MOF ($P_{CO2+H2S}$ = 1057.7 Barrer, $\alpha_{(CO2+H2S)/CH4}$ = 52.8) and 19 wt% Eu-naph-fcu-MOF ($P_{CO2+H2S}$ = 747.8 Barrer, $\alpha_{(CO2+H2S)/CH4}$ = 49.2).

Interestingly, after the $H_2S$ exposure for a period of 20–40 h, both $P_{CO2}$ and $\alpha_{CO2/CH4}$ of all membranes were regained to pre-$H_2S$ exposure values, indicating $H_2S$ presence only causes reversible competitive sorption between the permeating molecules, no $H_2S$-induced plasticization and no other permanent effect. Referring to the XRD patterns (Fig. 5), based on their characteristic diffraction peaks of Zr-MOF [80], we found that the MOF maintained their crystallinity phase in the polymer matrix, after $H_2S$-exposure (average $H_2S$-exposure time of 20–30 h). These remarkable results confirmed 6FDA-DAM and its Zr-MOF MMMs capability, effectiveness and stability for simultaneous acid gases separation from $CH_4$.

## 4. Conclusion

6FDA-DAM polyimide offers an attractive opportunity in gas separation application, and the incorporation of the highly stable zirconium-based UiO-66 and its functionalized derivatives as MMM further enhanced the separation properties. The membranes possessed excellent $CO_2/CH_4$ separation performance and presented high-performance stability at conditions relevant to actual gas processing (pressure, $CO_2$ content, temperature). The Zr-MOFs improved not only 6FDA-DAM gas separation properties but also deterred $CO_2$-induced plasticization and swelling. Additionally, in the presence of high $H_2S$ content (50,000 ppm in feed mixture) at high total pressure, both $CO_2$- and $H_2S$-induced plasticization were suppressed, and only reversible competitive sorption effect was observed. This successful high-pressure testing of 6FDA-DAM MMMs with Zr-MOFs is encouraging and

industrially relevant for natural gas sweetening at high pressure. Nevertheless, the separation understanding in the presence of water vapor and condensable hydrocarbons needs to be addressed beforehand. These impurities are not only suspected to reduce the separation performance but could also deteriorate the physical integrity of a membrane system.

## Acknowledgements

The research leading to these results has received funding from ECCSEL (Grant Agreement no. 675206, European Union's Horizon 2020 research and innovation programme). The authors also acknowledge the financial support of EACEA/European Commission, within the "Erasmus Mundus Doctorate in Membrane Engineering – EUDIME" (ERASMUS MUNDUS Programme 2009-2013, FPA n. 2011-0014, SGA n. 2012-1719), the Spanish Ministry of Economy and Competitiveness (MINECO), FEDER (MAT2016-77290-R), the European Social Fund and the Aragón Government (DGA, T05). Also the Operational Programme Prague–Competitiveness (CZ.2.16/3.1.00/24501) and National Program of Sustainability (NPU I LO1613) MSMT-43760/2015.

## Appendix A. Supplementary material

Supplementary data to this article can be found online at https://doi.org/10.1016/j.seppur.2019.115858.

## References

[1] S. Faramawy, T. Zaki, A.A.E. Sakr, Natural gas origin, composition, and processing: a review, J. Nat. Gas Sci. Eng. 34 (2016) 34–54, https://doi.org/10.1016/j.jngse.2016.06.030.
[2] B. Shimekit, H. Mukhtar, Natural gas purification technologies-major advances for $CO_2$ separation and future directions, Adv. Nat. Gas Technol. (2012) 235–270, https://doi.org/10.5772/38656.
[3] X.Y. Chen, H. Vinh-Thang, A.A. Ramirez, D. Rodrigue, S. Kaliaguine, Membrane gas separation technologies for biogas upgrading, RSC Adv. 5 (2015) 24399–24448, https://doi.org/10.1039/C5RA00666J.
[4] A. Kazemi, M. Malayeri, A. Gharibi Kharaji, A. Shariati, Feasibility study, simulation and economical evaluation of natural gas sweetening processes – Part 1: A case study on a low capacity plant in Iran, J. Nat. Gas Sci. Eng. 20 (2014) 16–22, https://doi.org/10.1016/j.jngse.2014.06.001.
[5] Z.A. Manan, W.N.R. Mohd Nawi, S.R. Wan Alwi, J.J. Klemeš, Advances in Process Integration research for $CO_2$ emission reduction – a review, J. Clean. Prod. 167 (2017) 1–13, https://doi.org/10.1016/j.jclepro.2017.08.138.
[6] E.D. Bates, R.D. Mayton, I. Ntai, J.H. Davis, $CO_2$ capture by a task-specific ionic liquid, J. Am. Chem. Soc. 124 (2002) 926–927, https://doi.org/10.1021/ja017593d.
[7] A.J. Kidnay, W.R. Parrish, Overview of natural gas industry, in: L.L. Faulkner (Ed.), Fundam. Nat. Gas Process. CRC Press, Taylor & Francis Group, Boca Raton, FL, 2006, pp. 1–21.
[8] M. Galizia, W.S. Chi, Z.P. Smith, T.C. Merkel, R.W. Baker, B.D. Freeman, 50th Anniversary perspective: polymers and mixed matrix membranes for gas and vapor separation: a review and prospective opportunities, Macromolecules (2017) 7809–7843, https://doi.org/10.1021/acs.macromol.7b01718.
[9] R.W. Baker, Vapor and gas separation by membranes, Adv. Membr. Technol. Appl. John Wiley & Sons, Inc., 2008, pp. 557–580, , https://doi.org/10.1002/9780470276280.ch21.
[10] T. Rodenas, I. Luz, G. Prieto, B. Seoane, H. Miro, A. Corma, F. Kapteijn, F.X. Llabrés i Xamena, J. Gascon, Metal–organic framework nanosheets in polymer composite materials for gas separation, Nat. Mater. 14 (2014) 48–55, https://doi.org/10.1038/nmat4113.
[11] N.L. Le, Y. Wang, T.S. Chung, Synthesis, cross-linking modifications of 6FDA-NDA/DABA polyimide membranes for ethanol dehydration via pervaporation, J. Memb. Sci. 415–416 (2012) 109–121, https://doi.org/10.1016/j.memsci.2012.04.042.
[12] K. Vanherck, G. Koeckelberghs, I.F.J. Vankelecom, Crosslinking polyimides for membrane applications: a review, Prog. Polym. Sci. 38 (2013) 874–896, https://doi.org/10.1016/j.progpolymsci.2012.11.001.
[13] J.D. Wind, C. Staudt-Bickel, D.R. Paul, W.J. Koros, Solid-state covalent cross-linking of polyimide membranes for carbon dioxide plasticization reduction, Macromolecules 36 (2003) 1882–1888, https://doi.org/10.1021/ma025938m.
[14] M.L. Chua, Y.C. Xiao, T.S. Chung, Modifying the molecular structure and gas separation performance of thermally labile polyimide-based membranes for enhanced natural gas purification, Chem. Eng. Sci. 104 (2013) 1056–1064, https://doi.org/10.1016/j.ces.2013.10.034.
[15] M.Z. Ahmad, H. Pelletier, V. Martin-Gil, R. Castro-Muñoz, V. Fila, Chemical crosslinking of 6FDA-ODA and 6FDA-ODA:DABA for improved $CO_2/CH_4$ separation, Membranes 8 (2018) 1–16, https://doi.org/10.3390/membranes8030067.
[16] W.F. Yong, K.H.A. Kwek, K.S. Liao, T.S. Chung, Suppression of aging and plasticization in highly permeable polymers, Polymer (Guildf) 77 (2015) 377–386, https://doi.org/10.1016/j.polymer.2015.09.075.
[17] R.T. Adams, J.S. Lee, T.H. Bae, J.K. Ward, J.R. Johnson, C.W. Jones, S. Nair, W.J. Koros, $CO_2$-$CH_4$ permeation in high zeolite 4A loading mixed matrix membranes, J. Memb. Sci. 367 (2011) 197–203, https://doi.org/10.1016/j.memsci.2010.10.059.
[18] S. Shahid, K. Nijmeijer, High pressure gas separation performance of mixed-matrix polymer membranes containing mesoporous Fe(BTC), J. Memb. Sci. 459 (2014) 33–44, https://doi.org/10.1016/j.memsci.2014.02.009.
[19] S. Akbar, A.H. Navarchian, Separation of carbon dioxide from natural gas through Matrimid-based mixed matrix membranes, Gas Process. J. 4 (2016) 1–18, https://doi.org/10.22108/gpj.2017.102840.1009.
[20] M.Z. Ahmad, V. Martin-gil, V. Perfilov, P. Sysel, V. Fila, Investigation of a new co-polyimide, 6FDA-bisP and its ZIF-8 mixed matrix membranes for $CO_2/CH_4$ separation, Sep. Purif. Technol. 207 (2018) 523–534, https://doi.org/10.1016/j.seppur.2018.06.067.
[21] T. Visser, G.H. Koops, M. Wessling, On the subtle balance between competitive sorption and plasticization effects in asymmetric hollow fiber gas separation membranes, J. Memb. Sci. 252 (2005) 265–277, https://doi.org/10.1016/j.memsci.2004.12.015.
[22] S. Lee, M. Binns, J.H. Lee, J.-H. Moon, J. Yeo, Y.-K. Yeo, Y.M. Lee, J.-K. Kim, Membrane separation process for $CO_2$ capture from mixed gases using TR and XTR hollow fiber membranes: process modeling and experiments, J. Memb. Sci. 541 (2017), https://doi.org/10.1016/j.memsci.2017.07.003.
[23] M. Scholz, T. Harlacher, T. Melin, M. Wessling, Modeling gas permeation by linking nonideal effects, Ind. Eng. Chem. Res. 52 (2013) 1079–1088, https://doi.org/10.1021/ie202689m.
[24] C.A. Scholes, G.W. Stevens, S.E. Kentish, The effect of hydrogen sulfide, carbon monoxide and water on the performance of a PDMS membrane in carbon dioxide/nitrogen separation, J. Memb. Sci. 350 (2010) 189–199, https://doi.org/10.1016/j.memsci.2009.12.027.
[25] M. Saberi, A.A. Dadkhah, S.A. Hashemifard, Modeling of simultaneous competitive mixed gas permeation and $CO_2$ induced plasticization in glassy polymers, J. Memb. Sci. 499 (2016) 164–171, https://doi.org/10.1016/j.memsci.2015.09.044.
[26] O.M. Yaghi, M. O'Keeffe, N.W. Ockwig, H.K. Chae, M. Eddaoudi, J. Kim, Reticular synthesis and the design of new materials, Nature 423 (2003) 705–714, https://doi.org/10.1038/nature01650.
[27] H.B. Tanh Jeazet, C. Staudt, C. Janiak, Metal–organic frameworks in mixed-matrix membranes for gas separation, Dalt. Trans. 41 (2012) 14003, https://doi.org/10.1039/c2dt31550e.
[28] X. Yan, S. Komarneni, Z. Zhang, Z. Yan, Extremely enhanced $CO_2$ uptake by HKUST-1 metal-organic framework via a simple chemical treatment, Micropor. Mesopor. Mater. 183 (2014) 69–73, https://doi.org/10.1016/j.micromeso.2013.09.009.
[29] A.R. Millward, O.M. Yaghi, Metal-organic frameworks with exceptionally high capacity for storage of carbon dioxide at room temperature, J. Am. Chem. Soc. 127 (2005) 17998–17999, https://doi.org/10.1021/ja0570032.
[30] O.K. Farha, I. Eryazici, N.C. Jeong, B.G. Hauser, C.E. Wilmer, A.A. Sarjeant, R.Q. Snurr, S.T. Nguyen, A.Ö. Yazaydin, J.T. Hupp, Metal-organic framework materials with ultrahigh surface areas: Is the sky the limit? J. Am. Chem. Soc. 134 (2012) 15016–15021, https://doi.org/10.1021/ja3055639.
[31] M. Zamidi Ahmad, M. Navarro, M. Lhotka, B. Zornoza, C. Téllez, V. Fila, J. Coronas, Enhancement of CO2/CH4 separation performances of 6FDA-based co-polyimides mixed matrix membranes embedded with UiO-66 nanoparticles, Sep. Purif. Technol. 192 (2018) 465–474, https://doi.org/10.1016/j.seppur.2017.10.039.
[32] V. Martin-Gil, A. Lopez, P. Hrabanek, R. Mallada, I.F.J. Vankelecom, V. Fila, Study of different titanosilicate (TS-1 and ETS-10) as fillers for Mixed Matrix Membranes for $CO_2/CH_4$ gas separation applications, J. Memb. Sci. 523 (2017) 24–35, https://doi.org/10.1016/j.memsci.2016.09.041.
[33] E.M. Mahdi, J.C. Tan, Mixed-matrix membranes of zeolitic imidazolate framework (ZIF-8)/Matrimid nanocomposite: thermo-mechanical stability and viscoelasticity underpinning membrane separation performance, J. Memb. Sci. 498 (2016) 276–290, https://doi.org/10.1016/j.memsci.2015.09.066.
[34] M.Z. Ahmad, M. Navarro, M. Lhotka, B. Zornoza, C. Téllez, W.M. De Vos, N.E. Benes, N.M. Konnertz, T. Visser, R. Semino, G. Maurin, V. Fila, J. Coronas, Enhanced gas separation performance of 6FDA-DAM based mixed matrix membranes by incorporating MOF UiO-66 and its derivatives, J. Memb. Sci. 558 (2018) 64–77, https://doi.org/10.1016/j.memsci.2018.04.040.
[35] R. Semino, J.C. Moreton, N.A. Ramsahye, S.M. Cohen, G. Maurin, Understanding the origins of metal–organic framework/polymer compatibility, Chem. Sci. 00 (2018) 1–10, https://doi.org/10.1039/C7SC04152G.
[36] Z. Li, F. Liao, F. Jiang, B. Liu, S. Ban, G. Chen, C. Sun, P. Xiao, Y. Sun, Capture of $H_2S$ and $SO_2$ from trace sulfur containing gas mixture by functionalized UiO-66(Zr) materials: a molecular simulation study, Fluid Phase Equilib. 427 (2016) 259–267, https://doi.org/10.1016/j.fluid.2016.07.020.
[37] M.W. Anjum, F. Vermoortele, A.L. Khan, B. Bueken, D.E. De Vos, I.F.J. Vankelecom, Modulated UiO-66-based mixed-matrix membranes for $CO_2$ separation, ACS Appl. Mater. Interf. 7 (2015) 25193–25201, https://doi.org/10.1021/acsami.5b08964.
[38] L. Hou, L. Wang, N. Zhang, Z. Xie, D. Dong, Polymer brushes on metal-organic frameworks by UV-induced photopolymerization, Polym. Chem. 7 (2016) 5828–5834, https://doi.org/10.1039/C6PY01008C.
[39] S.J. Garibay, S.M. Cohen, Isoreticular synthesis and modification of frameworks with the UiO-66 topology, Chem. Commun. (Camb.) 46 (2010) 7700–7702, https://doi.org/10.1039/c0cc02990d.
[40] S. Basu, A. Cano-Odena, I.F.J. Vankelecom, MOF-containing mixed-matrix membranes for $CO_2/CH_4$ and $CO_2/N_2$ binary gas mixture separations, Sep. Purif.

Technol. 81 (2011) 31–40, https://doi.org/10.1016/j.seppur.2011.06.037.
[41] S.A. Hashemifard, A.F. Ismail, T. Matsuura, Prediction of gas permeability in mixed matrix membranes using theoretical models, J. Memb. Sci. 347 (2010) 53–61, https://doi.org/10.1016/j.memsci.2009.10.005.
[42] P.S. Goh, A.F. Ismail, S.M. Sanip, B.C. Ng, M. Aziz, Recent advances of inorganic fillers in mixed matrix membrane for gas separation, Sep. Purif. Technol. 81 (2011) 243–264, https://doi.org/10.1016/j.seppur.2011.07.042.
[43] A. Perea-Cachero, J. Sánchez-Laínez, Á. Berenguer-Murcia, D. Cazorla-Amorós, C. Téllez, J. Coronas, A new zeolitic hydroxymethylimidazolate material and its use in mixed matrix membranes based on 6FDA-DAM for gas separation, J. Memb. Sci. 544 (2017) 88–97, https://doi.org/10.1016/j.memsci.2017.09.009.
[44] B.D. Freeman, Basis of permeability/selectivity tradeoff relations in polymeric gas separation membranes, Macromolecules 32 (1999) 375–380, https://doi.org/10.1021/ma9814548.
[45] S. Shahid, K. Nijmeijer, Performance and plasticization behavior of polymer-MOF membranes for gas separation at elevated pressures, J. Memb. Sci. 470 (2014) 166–177, https://doi.org/10.1016/j.memsci.2014.07.034.
[46] B. Zornoza, C. Tellez, J. Coronas, J. Gascon, F. Kapteijn, Metal organic framework based mixed matrix membranes: an increasingly important field of research with a large application potential, Micropor. Mesopor. Mater. 166 (2013) 67–78, https://doi.org/10.1016/j.micromeso.2012.03.012.
[47] H. Lin, M. Yavari, Upper bound of polymeric membranes for mixed-gas $CO_2/CH_4$ separations, J. Memb. Sci. 475 (2015) 101–109, https://doi.org/10.1016/j.memsci.2014.10.007.
[48] O.G. Nik, X.Y. Chen, S. Kaliaguine, Functionalized metal organic framework-polyimide mixed matrix membranes for $CO_2/CH_4$ separation, J. Memb. Sci. 413–414 (2012) 48–61, https://doi.org/10.1016/j.memsci.2012.04.003.
[49] S. Castarlenas, C. Tellez, J. Coronas, Gas separation with mixed matrix membranes obtained from MOF UiO-66-graphite oxide hybrids, J. Memb. Sci. 526 (2017) 205–211, https://doi.org/10.1016/j.memsci.2016.12.041.
[50] V. Stannett, The transport of gases in synthetic polymeric membranes - an historic perspective, J. Memb. Sci. 3 (1978) 97–115, https://doi.org/10.1016/S0376-7388(00)83016-1.
[51] J.E. Bachman, Z.P. Smith, T. Li, T. Xu, J.R. Long, Enhanced ethylene separation and plasticization resistance in polymer membranes incorporating metal–organic framework nanocrystals, Nat. Mater. 15 (2016) 845–849, https://doi.org/10.1038/nmat4621.
[52] B. Zornoza, C. Téllez, J. Coronas, O. Esekhile, W.J. Koros, Mixed matrix membranes based on 6FDA polyimide with silica and zeolite microsphere dispersed phases, AIChE J. 61 (2015) 4481–4490, https://doi.org/10.1002/aic.15011.
[53] W. Ogieglo, M. Wessling, N.E. Benes, Polymer relaxations in thin films in the vicinity of a penetrant- or temperature-induced glass transition, Macromolecules 47 (2014) 3654–3660, https://doi.org/10.1021/ma5002707.
[54] J.S. Vrentas, C.M. Vrentas, Sorption in glassy polymers, Macromolecules 24 (1991) 2404–2412, https://doi.org/10.1021/ma00009a043.
[55] F. Doghieri, G.C. Sarti, Nonequilibrium lattice fluids: a predictive model for the solubility in glassy polymers, Macromolecules 29 (1996) 7885–7896, https://doi.org/10.1021/ma951366c.
[56] R. Swaidan, B. Ghanem, E. Litwiller, I. Pinnau, Effects of hydroxyl-functionalization and sub-Tg thermal annealing on high pressure pure- and mixed-gas $CO_2/CH_4$ separation by polyimide membranes based on 6FDA and triptycene-containing dianhydrides, J. Memb. Sci. 475 (2015) 571–581, https://doi.org/10.1016/j.memsci.2014.10.046.
[57] R. Heck, M.S. Qahtani, G.O. Yahaya, I. Tanis, D. Brown, A.A. Bahamdan, A.W. Ameen, M.M. Vaidya, J.P.R. Ballaguet, R.H. Alhajry, E. Espuche, R. Mercier, Block copolyimide membranes for pure- and mixed-gas separation, Sep. Purif. Technol. 173 (2017) 183–192, https://doi.org/10.1016/j.seppur.2016.09.024.
[58] L.M. Robeson, The upper bound revisited, J. Memb. Sci. 320 (2008) 390–400, https://doi.org/10.1016/j.memsci.2008.04.030.
[59] W.J. Koros, R.T. Chern, V. Stannett, H.B. Hopfenberg, A model for permeation of mixed gases and vapors in glassy polymers, J. Polym. Sci. Polym. Phys. Ed. 19 (1981) 1513–1530, https://doi.org/10.1002/pol.1981.180191004.
[60] U. Cakal, L. Yilmaz, H. Kalipcilar, Effect of feed gas composition on the separation of $CO_2/CH_4$ mixtures by PES-SAPO 34-HMA mixed matrix membranes, J. Memb. Sci. 417–418 (2012) 45–51, https://doi.org/10.1016/j.memsci.2012.06.011.
[61] J.H. Kim, W.J. Koros, D.R. Paul, Effects of $CO_2$ exposure and physical aging on the gas permeability of thin 6FDA-based polyimide membranes. Part 1. Without crosslinking, J. Memb. Sci. 282 (2006) 21–31, https://doi.org/10.1016/j.memsci.2006.05.004.
[62] L. Cui, W. Qiu, D.R. Paul, W.J. Koros, Responses of 6FDA-based polyimide thin membranes to $CO_2$ exposure and physical aging as monitored by gas permeability, Polymer (Guildf). 52 (2011) 5528–5537, https://doi.org/10.1016/j.polymer.2011.10.008.
[63] S. Sridhar, B. Smitha, T.M. Aminabhavi, Separation of carbon dioxide from natural gas mixtures through polymeric membranes – a review, Sep. Purif. Rev. 36 (2007) 113–174, https://doi.org/10.1080/15422110601165967.
[64] E.V. Perez, K.J. Balkus, J.P. Ferraris, I.H. Musselman, Mixed-matrix membranes containing MOF-5 for gas separations, J. Memb. Sci. 328 (2009) 165–173, https://doi.org/10.1016/j.memsci.2008.12.006.
[65] A. Bos, I.G.M. Pünt, M. Wessling, H. Strathmann, $CO_2$-induced plasticization phenomena in glassy polymers, J. Memb. Sci. 155 (1999) 67–78, https://doi.org/10.1016/S0376-7388(98)00299-3.
[66] T. Battal, N. Baç, L. Yilmaz, Effect of feed composition on the performance of polymer-zeolite mixed matrix gas separation membranes, Sep. Sci. Technol. 30 (1995) 2365–2384, https://doi.org/10.1080/01496399508013117.
[67] T. Komatsuka, K. Nagai, Temperature dependence on gas permeability and permselectivity of poly(lactic acid) blend membranes, Polym. J. 41 (2009) 455–458, https://doi.org/10.1295/polymj.PJ2008266.
[68] R.P. Singh, X. Li, K.W. Dudeck, B.C. Benicewicz, K.A. Berchtold, Polybenzimidazole based random copolymers containing hexafluoroisopropylidene functional groups for gas separations at elevated temperatures, Polymer (Guildf). 119 (2017) 134–141, https://doi.org/10.1016/j.polymer.2017.04.075.
[69] L.A. Kareem, T.M. Iwalewa, M. Al-Marhoun, New explicit correlation for the compressibility factor of natural gas: linearized z-factor isotherms, J. Pet. Explor. Prod. Technol. 6 (2016) 481–492, https://doi.org/10.1007/s13202-015-0209-3.
[70] J. Sánchez-Laínez, B. Zornoza, S. Friebe, J. Caro, S. Cao, A. Sabetghadam, B. Seoane, J. Gascon, F. Kapteijn, C. Le Guillouzer, G. Clet, M. Daturi, C. Téllez, J. Coronas, Influence of ZIF-8 particle size in the performance of polybenzimidazole mixed matrix membranes for pre-combustion $CO_2$ capture and its validation through interlaboratory test, J. Memb. Sci. 515 (2016) 45–53, https://doi.org/10.1016/j.memsci.2016.05.039.
[71] D.W. Van Krevelen, K. Te Nijenhuis, Chapter 7 – Cohesive properties and solubility, in: D.W. Van Krevelen, K. Te Nijenhuis (Eds.), Prop. Polym., fourth ed., Elsevier, Amsterdam, 2009, pp. 189–227. doi: 10.1016/B978-0-08-054819-7.00007-8.
[72] A. Kazemi, A.G. Kharaji, A. Mehrabani-Zeinabad, V. Faizi, J. Kazemi, A. Shariati, Synergy between two natural gas sweetening processes, J. Unconv. Oil Gas Resour. 14 (2016) 6–11, https://doi.org/10.1016/j.juogr.2016.01.002.
[73] A.A. Radzig, B.M. Smirnov, Interaction potentials between atomic and molecular species, in: Ref. Data Atoms, Mol. Ions. Springer Ser. Chem. Phys., Springer, Berlin, Heidelberg, 1985, pp. 317–315. doi: 10.1007/978-3-642-82048-9_9.
[74] J. Vaughn, W.J. Koros, Effect of the amide bond diamine structure on the CO2, H2S, and CH4 transport properties of a series of novel 6FDA-based polyamide-imides for natural gas purification, Macromolecules 45 (2012) 7036–7049, https://doi.org/10.1021/ma301249x.
[75] G.O. Yahaya, M.S. Qahtani, A.Y. Ammar, A.A. Bahamdan, A.W. Ameen, R.H. Alhajry, M.M.B. Sultan, F. Hamad, Aromatic block co-polyimide membranes for sour gas feed separations, Chem. Eng. J. 304 (2016) 1020–1030, https://doi.org/10.1016/j.cej.2016.06.076.
[76] T. Mohammadi, M.T. Moghadam, M. Saeidi, M. Mahdyarfar, Acid gas permeation behavior through poly (ester urethane urea) membrane, Ind. Eng. Chem. Res. 47 (2008) 7361–7367.
[77] G. Chatterjee, A.A. Houde, S.A. Stern, Poly(ether urethane) and poly(ether urethane urea) membranes with high $H_2S/CH_4$ selectivity, J. Memb. Sci. 135 (1997) 99–106, https://doi.org/10.1016/S0376-7388(97)00134-8.
[78] S.M.S. Niknejad, H. Savoji, M. Pourafshari Chenar, M. Soltanieh, Separation of $H_2S$ from $CH_4$ by polymeric membranes at different $H_2S$ concentrations, Int. J. Environ. Sci. Technol. 14 (2017) 375–384, https://doi.org/10.1007/s13762-016-1156-3.
[79] G. Liu, V. Chernikova, Y. Liu, K. Zhang, Y. Belmabkhout, O. Shekhah, C. Zhang, S. Yi, M. Eddaoudi, W.J. Koros, Mixed matrix formulations with MOF molecular sieving for key energy-intensive separations, Nat. Mater. 17 (2018) 283–289, https://doi.org/10.1038/s41563-017-0013-1.
[80] L. Valenzano, B. Civalleri, S. Chavan, S. Bordiga, M.H. Nilsen, S. Jakobsen, K.P. Lillerud, C. Lamberti, Disclosing the complex structure of UiO-66 metal organic framework: a synergic combination of experiment and theory, Chem. Mater. 23 (2011) 1700–1718, https://doi.org/10.1021/cm1022882.
[81] S. Yi, X. Ma, I. Pinnau, W.J. Koros, A high-performance hydroxyl-functionalized polymer of intrinsic microporosity for an environmentally attractive membrane-based approach to decontamination of sour natural gas, J. Mater. Chem. A. 3 (2015) 22794–22806, https://doi.org/10.1039/C5TA05928C.
[82] B. Kraftschik, W.J. Koros, J.R. Johnson, O. Karvan, Dense film polyimide membranes for aggressive sour gas feed separations, J. Memb. Sci. 428 (2013) 608–619, https://doi.org/10.1016/j.memsci.2012.10.025.